Damage Identification in Masonry Structures with Vibration Measurements

L.F. Ramos & P.B. Lourenço
ISISE, University of Minho, Guimarães, Portugal, lramos@civil.uminho.pt

G. De Roeck
Catholic University of Leuven, Belgium

A. Campos-Costa
LNEC, Lisbon, Portugal

ABSTRACT: The paper aims at exploring damage assessment in masonry structures at an early stage by vibration measurements. For this purpose, one approach is proposed combining global and local ND methods. To further evaluate the approach, one masonry tower in Portugal was studied together with one wall model in the laboratory. The model was built as reference, undamaged, state. Afterwards, progressive damage was induced and sequential modal identification analysis was performed at each damage stage, aiming to find adequate correspondence between dynamic behavior and internal crack growth. The paper presents all the analyses carried out with the aim to detect and locate the damage by means of vibrations measurements.

1 INTRODUCTION

Damage on masonry structures mainly relates to cracks, foundation settlements, material degradation and displacements. When cracks occur, generally they are localized, splitting the structures in macro-blocks. Dynamic based methods to assess the damage are attractive to this type of structures due to the present requirements of unobtrusiveness, minimum physical intervention and respect of the original construction. The assumption that damage can be linked to a decrease of stiffness also seems to be reasonable to this type of structures.

The present paper deals with the problem of damage identification by using Global and Local damage identification techniques. It is advantageous to have two categories for damage identification: (a) the vibration based damage identification methods, currently defined as Global methods, because they do not give sufficiently accurate information about the extent of the damage, but they can identify its presence and define its precise location (e.g. Chang et al., 2003); and (b) the methods based on visual inspections or experimental tests, such as sonic tests, radar tests, radiograph and thermal field methods (e.g. Doherty, 1987), also called as Local methods.

Many methods are presented in literature for damage identification based on vibration signatures, see Montalvão et al. (2006), but there are only a few papers on the application to masonry like structures. An important task before damage can be identified from vibration characteristics is the study and subsequent elimination of the environmental effects Peeters (2000).

2 PROPOSED APPROACH FOR DAMAGE IDENTIFICATION

The current practice of structural health monitoring is based mainly on periodic visual inspections or condition surveys but, during the last decade, software and hardware developments made continuous monitoring possible, Chang et al. (2003). Typically, one can install hundreds of sensors in a structure and read the data in real time. Therefore, the present focus of interest is what type of information is important from the structural point of view and how should the data be processed and stored for damage analysis, Londoño (2006)?

Given the latest advantages in the field of damage identification analysis and concerning monitoring, it is proposed to monitor historical masonry structures in four phases (Ramos, 2007):

1. The first phase is the data collection of the structure, including the historical information, geometrical and topographic survey, damage survey, the mechanical characterization of materials with Non Destructive (ND) tests, a global dynamic modal test and a numerical model analysis for static and dynamic calibration. This is the first approach to the structural behaviour in the assumed healthy condition at time “zero”;
2. In the second phase the health monitoring plan can resort to a limited number of sensors (e.g. a pair of reference accelerometers, strain gauges at critical sections, tem-

perature and humidity sensors, etc). Data should be stored periodically and the monitoring system should be able to send an alarm. Environmental and loading effects should be studied and the presence of damage should be detected by the global modal parameters;

3. In the third phase, after alarm triggering, a full-scale dynamic survey with more sensors and measuring points should be performed. In this phase the "health condition" of a structure is studied with more detail. Damage identification methods should be applied to the structure after filtering the environmental effects. The aim of the dynamic methods is to confirm and locate the (possible) damage in a global way;
4. In the last phase, a local approach with visual and complementary ND tests should be performed to locally assess the damage and classify it. This can be carried out with sonic test or radar tests, depending on the access conditions of the structure. This local approach can give a better definition of damage.

The global and local approach should be considered as complementary tasks. For the case of historical constructions these two approaches seem to be suitable, since they are ND procedures to evaluate the health conditions.

The following sessions present one case study and one laboratory simulation of the University of Minho, where the first three phases of the preceding methodology were already applied.

3 STRUCTURAL ASSESSMENT

For the first phase of the proposed approach it is presented the case study of Mogadouro Clock Tower. The Mogadouro Clock Tower is located inside the castle perimeter of Mogadouro (see Figure 1), a small town in the Northeast of Portugal. It has a rectangular cross section of 4.7×4.5 m^2 with and interior hole of 2.5×2.3 m^2, and a height equal to 20.4 m. It was built in stone masonry with granite and shale, with dry joints at the corners and with mortar joints in the central part of the walls. The walls have, on average, 1 m of thickness and are composed by an irregular bond of stones.

Due to lack of maintenance, severe damage was observed in the tower in 2004. The damage was characterized by cracks, material degradation, out-of-plane displacements, loss of material in some parts, and biological growth, see Figure 1a. The most severe damage was a pair of cracks in the East and West façade, see Figure 1b, that divided the box cross section of the tower in two separated U bodies, leading to a lower safety condition.

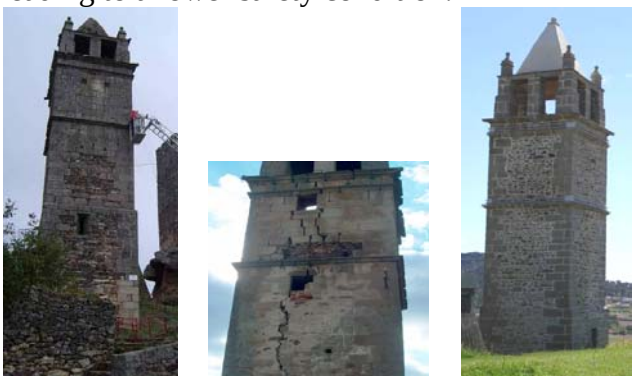

(a) (b) (c)

Figure 1 – Mogadouro Clock Tower: (a) and (b) general view of the tower with severe damage; and (c) the tower after the strengthening works

A geometrical survey of the structure with photogrammetry software allowed registering all anomalies and dimensions. The dimensions of the structural survey have an error about ±5 cm.

To re-establish the tower safety, consolidation works were carried out in 2005. The remedial treatment included: injections for the walls consolidation, replacement of deteriorated materials and the installation of tie-rods at two levels with very light prestressing stress. Figure 1c presents the final appearance of the tower after strengthening.

3.1 *Modal Identification Before and After the Rehabilitation Works*

In the case of the Mogadouro Tower, damage was evident and a dynamic based damage identification analysis to detect its presence was not necessary. Nevertheless, the dynamic based methods could be used to locate and to assess the damage. Therefore, two dynamic modal identification tests were performed before and after the structural rehabilitation. The aim was to compare the response of the tower with different structural conditions in order to localize the damage, to archive qualitatively the extent of damage present before the rehabilitation works, and to evaluate the efficiency of the rehabilitation works.

Table 1 and Figure 2 present frequencies and mode shapes, as well the Modal Assurance Criteria (MAC) values, for the two structural conditions. On average, the frequencies increase 50%.

Table 1 – Estimated natural frequencies values

Mode Shape	Before ω [Hz]	Before CV_ω [%]	After ω [Hz]	After CV_ω [%]	Δ_ω [%]
1st	2.15	1.85	2.56	0.21	+19.28
2nd	2.58	1.05	2.76	0.30	+6.70
3rd	4.98	0.69	7.15	0.27	+43.67
4th	5.74	1.56	8.86	0.47	+54.37
5th	6.76	1.13	9.21	0.21	+36.13
6th	7.69	2.94	15.21	2.24	+97.87
7th	8.98	1.21	16.91	1.40	+88.27

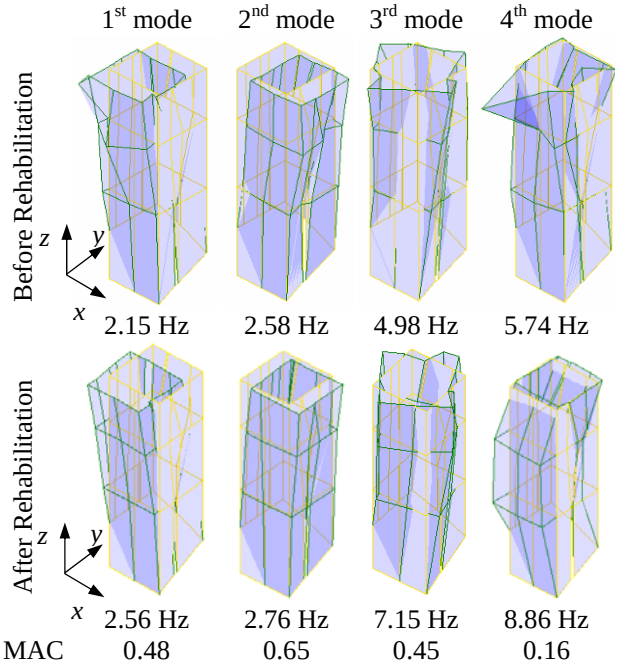

Figure 2 – Estimated mode shapes before and after strengthening, together with the MAC values

Analyzing the modal displacements, local protuberances can be observed in the areas close to the cracks and in the upper part before the rehabilitation. This is due to the presence of severe damage. The structure only behaves monolithically after the rehabilitation.

The global parameter results are consistent with the two structural conditions, i.e. the structure after rehabilitation has a new and higher stiffness.

3.2 *Numerical Modeling*

Aiming at a better understanding of the two structural conditions and to better evaluate the efficiency of the strengthening, FE analyses were also addressed. The numerical structural assessment was carried out by the application of the FE Model Updating method (FEMU). The nonlinear least square method implemented in MatLab (2006), function `lsqnonlin`, was used together with FE package DIANA (2006) to compute the numerical modes. The objective function π to be minimized is composed by the residuals formed with calculated and experimental frequencies and mode shapes, given by:

$$\pi = \frac{1}{2}\left[\sum_{j=1}^{m_\omega} W_\omega \left(\frac{\omega_j^2 - \omega_{j,\exp}^2}{\omega_{j,\exp}^2}\right)^2 + \sum_{j=1}^{m_\varphi} W_\varphi \left(\varphi_j - \varphi_{j,\exp}\right)^2\right] \quad (1)$$

where m_ω denotes the number of eigen frequencies taken into account, m_φ is the number of normalized eigen modes taken into account and W_ω and W_φ are weighting diagonal matrices for the frequencies and mode shapes, respectively. Note that in Eq.(1) experimental and numerical mode shapes are normalized in a way that the maximum real value of the modal displacement is equal to one, in order to be comparable with the residuals from the frequency values normalized by the experimental results.

A 3D model with brick (20 noded) elements was prepared. The model is presented in Figure 3 with the selected updating parameters (Young's modulus). The planar roof surfaces were modeled with 6 noded shell elements to simplify the mesh.

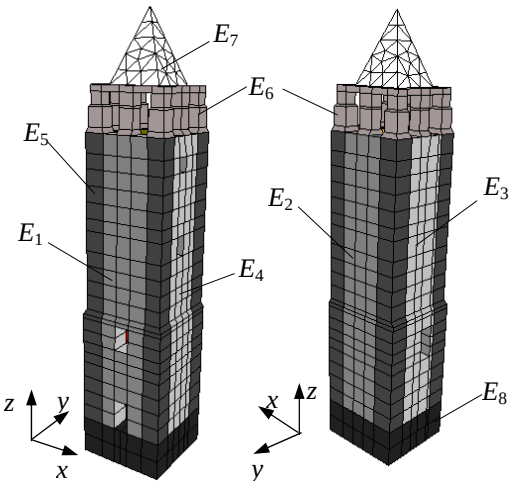

Figure 3 – Selected updating parameters

Table 2 presents the final results together with the difference and the relative values of the updating parameters. All the updating variables suffered a significant increase, with exception of the material at the corners (E_5), at the foundation (E_8), and at the North wall (E_2). For the corners and for the foundation these results are acceptable because the stone masonry at the corners was better than in the central parts of the walls, and the foundation material tries to represent not only the structural element but also the boundary conditions at the base. For the North wall a Young's modulus increase was expected, but in the strengthened condition the North wall had a higher Young's modulus, which might indicate that the wall was in better condition than the others. The others updating variables on average they increased three times the initial value.

Table 2 – Results of the updating analysis

Updating Parameters	Before [GPa]	After [GPa]	Diff. [GPa]	Relative Values
E_1 [GPa]	0.687	1.974	+1.287	2.87
E_2 [GPa]	2.210	2.210	–	1.00
E_3 [GPa]	0.302	1.075	+0.773	3.56
E_4 [GPa]	0.276	0.804	+0.528	2.91
E_5 [GPa]	3.870	3.875	+0.005	1.00
E_6 [GPa]	0.380	1.210	+0.830	3.18
E_7 [GPa]	0.083	0.195	+0.112	2.35
E_8 [GPa]	5.997	5.997	–	1.00

The results indicate that the damage on the tower was severe on the central parts of the South, East and West façades and at the upper part of the tower. These areas in the structure are the ones which suffer large mortar loss due to deterioration, meaning

that the results can be acceptable. Finally, one can conclude that the strengthening works were efficient at re-establishing the tower safety.

4 MONITORING TASK

The second phase of the proposed approach is the dynamic monitoring task, which can be performed with a limited number of sensors. This task has been carried out since April, 2006, in the Mogadouro Clock Tower. The aim is to evaluate the environmental and loading effects and to detect any possible non stabilized phenomena in the structure (damage), by studying the global dynamic parameters.

A low-cost monitoring system was chosen for this task. The system is composed by three piezoelectric accelerometers, connected by coaxial cables to a USB data acquisition card with 24 bits resolution, provided with anti-aliasing filters, which is connected to a Pentium II® laptop with an uninterruptible power supply device.

Two points (A1 and A2) were selected in the middle of Level 2 to acquire accelerations in three directions, see Figure 4a and b. In this way, all the mode shape components of the first five eigenfrequencies can be studied, including the torsion mode. The environmental measurements are acquired in the point TH, close to the datalogger (D).

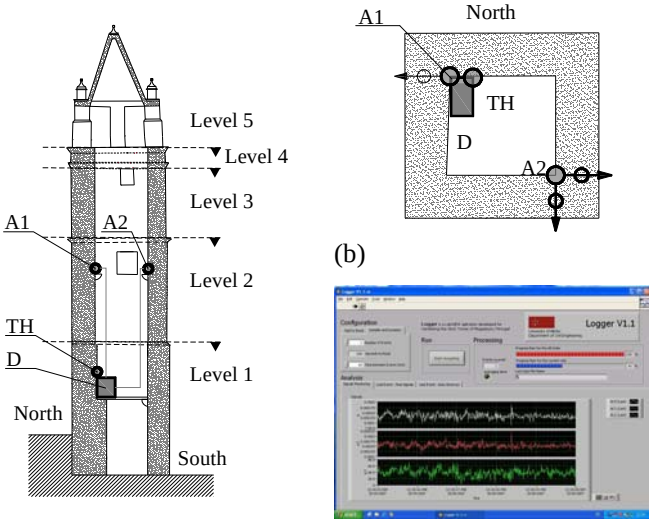

Figure 4 – Monitoring system: (a) and (b) sensors location; and (c) logger software

The LabView (2006) software was used to measure and acquire accelerations, see Figure 4c. In parallel, a combined sensor connected to the laptop through serial cable is recording the ambient temperature and relative air humidity. The environmental data is acquired in the laptop by interface software provided by the supplier of the combined sensor.

Every hour, 10 minutes of ambient vibrations in the three channels with a sampling frequency of 100 Hz are acquired without any triggering. The data is then saved in ASCII files.

Finally and for modal estimation, an automatic procedure based on SSI/Ref method (Peeters and De Roeck, 1999) was implemented in MatLab.

4.1 *Filtering the Environmental and Loading Effects for Damage Detection*

The study of the environmental and loading effects was initially based on the assumption that the modal response is changed by three independent variables: temperature, relative air humidity and the level of excitation. For the later and for every event, it was decided to use the average Root Mean Square (RMS) value of the three acceleration channels.

In general, there is a positive relation between temperature and frequency, and a negative relation between humidity and frequency and between level of excitation and frequency.

Here it should be stressed that a significant frequency shift related to the walls water absorption happens twice a year. Figure 5 presents the first resonant frequency variation compared with the environmental variables along short period. During this period the temperature did not change significantly, while the relative air humidity after 18th of October is close to 100%, i.e. the first raining season on the site. After 22nd of October the frequency values decrease linearly with humidity almost constant. This indicates that the structure absorbs water and the mass changes, reducing the frequency values because the two quantities are inverse related. It can also occur that water leads to a stiffness reduction, at least in the lime mortars. The inverse drying phenomenon also happens during the hot period.

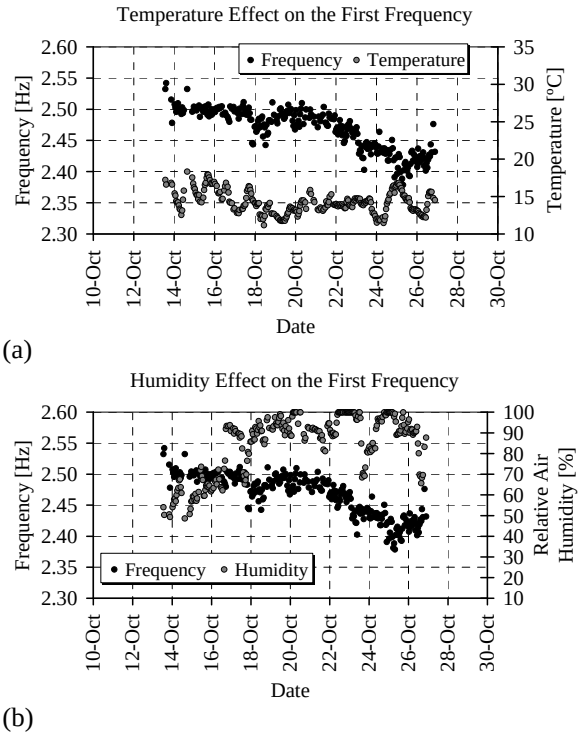

Figure 5 – Environmental effects of the dynamic response

Since the environmental and the loading variables are changing the modal parameters of the tower, an attempt to model the dynamic response according to the three variables was carried out. It was decided to use a procedure similar to the one used by Peeters (2000) with AutoRegressive output with an eXogeneous input parts models (ARX models). Here, ARX models with multiple inputs and a single output (MISO models) were computed in MatLab (2006), function `arx`, to model each frequency value. The multivariable ARX model with *n* inputs *u* and one output *y* is presented by:

$$A_q \hat{y}_k = B_q u_{k-nk}^{env} + e_k \quad (2)$$

where A_q is a scalar with the delay operator q^{-1}, B_q is a matrix $1 \times n$, and e is the unknown residuals. For damage detection, confidence intervals were establish and by analyzing the outliers is possible to detect damage.

Figure 6 shows for the first natural frequency the fitting model through the normalized frequency and simulated errors with the 95% confidence intervals *ci*. In general, the model represents the frequency variation, but it doesn't account the water absorption phenomenon, because the relative humidity variation does not totally represent that change. Furthermore, the damage is detected by frequency shifts that significantly go outside the confident intervals *ci*.

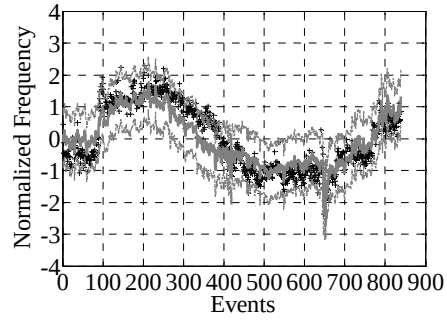

(a)

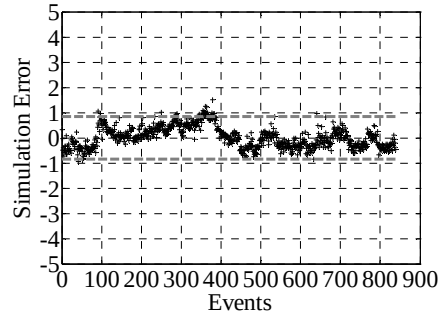

(b)

Figure 6 – Numerical simulation: (a) ARX model; and (b) the residuals distribution

Concerning the numerical frequency simulation, it should be stressed that the calibration period of one year might be not enough for having a tuned model. A longer period of, at least, three years should be used for calibration in order to have a reliable model for frequency prediction.

5 DAMAGE LOCALIZATION

For damage localization (the third phase of the proposed approach) a laboratory simulation of a wall model is presented here. The replicate of historical constructions was built as reference, undamaged, state. Afterwards, progressive damage was induced and sequential modal identification analysis was performed at each damage stage, aiming at finding adequate correspondence between dynamic behavior and internal crack growth.

The wall model was built with clay bricks with $210 \times 105 \times 55$ mm^3, handmade in the Northern area of Portugal. The adopted clay bricks have low compression strength and the adopted Mapei® mortar for the joints has low mechanical properties for the joints, trying to be representative of the materials used in the historical constructions. The wall has a length equal to 1.08 m, a height equal to 1.10 m, and a thickness equal to 0.105 m, which matches the bricks thickness, see Figure 7. The thickness of the joints is about 1.0 cm.

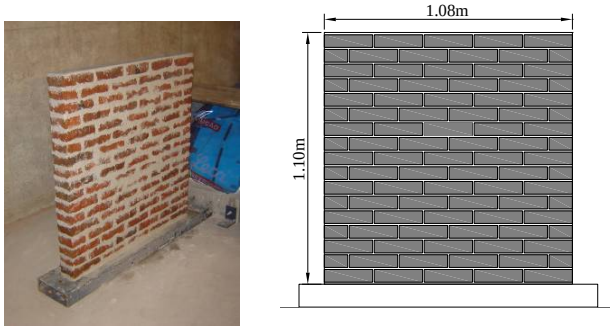

(a) (b)

Figure 7 – Wall model: (a) general view; and (b) dimensions

5.1 *Static Tests*

Fourteen Damage Scenarios (DS) were induced with the application of two static forces: a constant vertical force to replicate existing vertical compressive stresses and a horizontal force to produce shear stresses. The vertical load was transmitted through a group of three steel beams with appropriate devices to distribute uniformly the load to the wall. The last beam was direct glued to the wall. The in-plane stresses were applied with the aim of producing bending and shear cracks, i.e. to reproduce the common crack pattern present in the masonry piers that suffer earthquake actions.

To achieve several controlled cracks, three series of static tests were carried out. Figure 8 presents foo the last series (Series C) the test apparatus, the static response of the wall and the final crack pattern. From the static response is possible to observe the stiffness decrease, where the horizontal displacement indicated corresponds to the maximum or top value (LVDT 1).

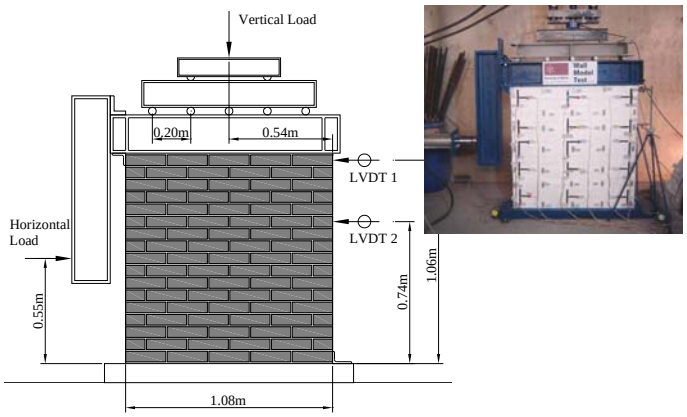

(a)

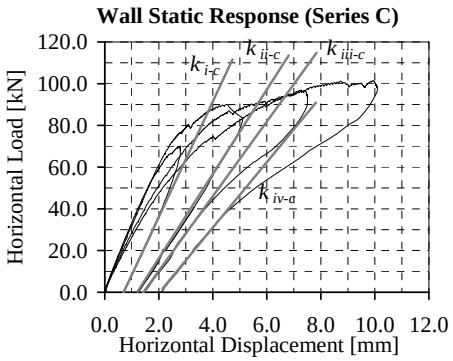

(b)

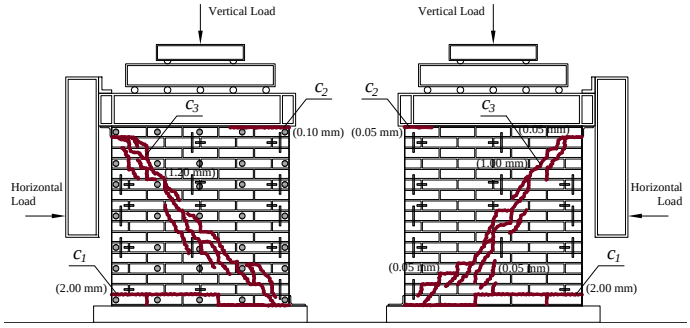

(c)

Figure 8 – Wall static tests: (a) test apparatus; (b) static response of the last series of tests; and (c) final crack pattern from the front and back sides of the wall

The final crack pattern includes three cracks. One bending crack is at left bottom part, and another bending crack is at right top part of the wall, namely crack c_1 and c_2, respectively. The third crack (c_3) is a shear crack in the diagonal direction of the wall.

5.2 *Dynamic Tests*

Between each DS, modal identification analysis using output-only techniques was performed. The selected sensors for the dynamic tests were the accelerometers and strain gauges with quarter bridge configuration. The strain gauges were selected to measure modal strains in order to directly estimate modal curvatures, which are quantities more sensitive to damage than the modal displacements (Ramos, 2007).

A regular grid of five vertical lines and seven horizontal lines was chosen for the accelerometers. In the case of the strains gauges, it was decided to use an array of three vertical lines and five horizontal lines. Figure 9 shows the location of the measuring points where the reference points are given in a grey box.

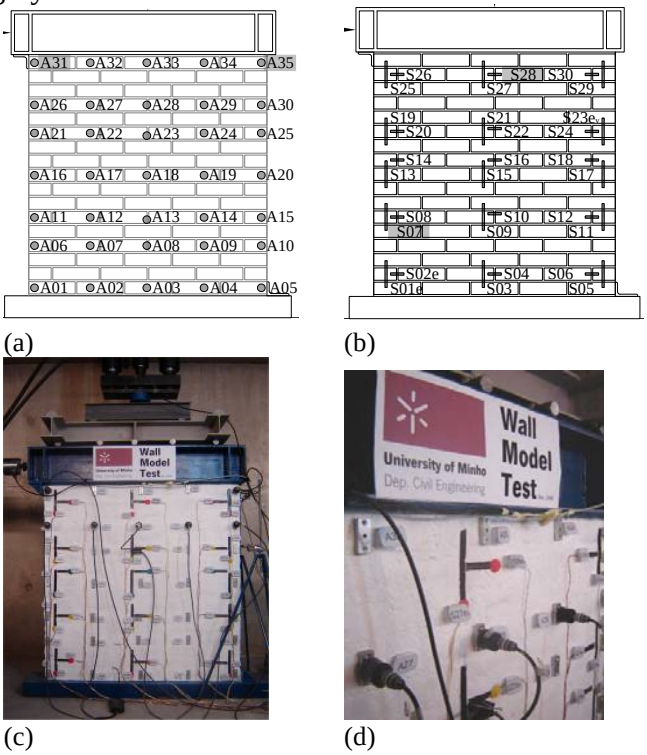

(a) (b)

(c) (d)

Figure 9 – Wall dynamic tests: (a) and (b) accelerometers and strain gauges locations, respectively; and (c) and (d) details of the ambient dynamic tests

The accelerometers were bolted to aluminum plates that were directly glued to the wall. The vertical strain gauges have 12 cm of length and the horizontal strain gauges have 6 cm of length. This way, the vertical strain gauge crosses, at least, three joints and the horizontal strain gauge only one joint.

Two different excitation types were used during the identification tests: (a) natural and ambient noise present in the laboratory; and (b) random impact excitation in space and in time with a hammer. The second excitation type was used because it was impossible to estimate accurately modal curvatures with ambient excitation. The impact forces were about 2% of the specimen mass.

The long-term changes of the environmental effects inside the laboratory where also studied. Figure 10 presents the average values for ambient and surface temperature and relative air humidity measured for each DS. The average temperature values were about 17ºC with a low increasing trend. The average humidity is about 69% with ±7% of maximum amplitude. Compared with the values obtained in the Mogadouro Clock Tower, it is expected for values of that order that the dynamic response of the wall does not change significantly and therefore it is assumed that the environmental effects inside the laboratory can be neglected in the subsequent damage identification analysis.

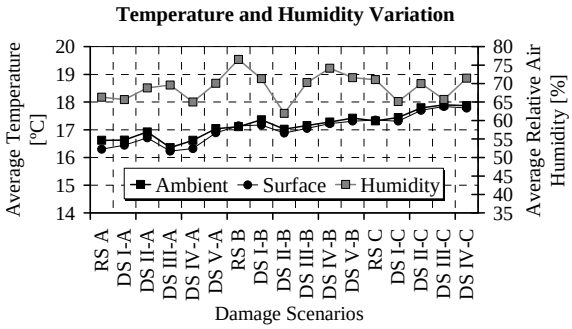

Figure 10 – Environmental effects inside the laboratory

5.3 *Damage Analysis*

For damage detection, the analysis was carried out by observing frequency sifts in the natural resonant frequencies. In the case of the damage localization analysis, a group of damage methods was selected aiming at providing an adequate approach for analysis. The selected methods are (see Doebling et al., 1996, and Montalvão et al., 2006, for details):

- The COMAC values;
- The Parameter Method (PM);
- The Mode Shape Curvature Method (MSCM);
- The Damage Index Method (DIM);
- The Sum of all Curvature Errors method (SCE);
- The FE Model Updating method (FEMU).

The selection of a group of methods can be discussible. Up to now, there is no single method which gives accurate results for damage localization and for all types of structural systems (Farrar and Doebling, 1998; and Choi et al., 2005). Therefore, the main issue is to obtain a wide perspective of the problem and conclusions on damage identification, taking into account that different methods provide different results. If significant damage is present in the structure, the results provided from different methods would converge in the identification, giving more confidence to the analyst.

All the selected methods have one common aspect: they all use spatial modal information of the structure, through mass-scaled or non-scaled mode shapes ϕ and φ, respectively (or/and through mass-scaled or non-scaled curvatures mode shapes ϕ'' and φ'', respectively). As damage is a local phenomenon, these quantities are useful to locate damage, especially the modal curvatures.

5.3.1 *Global Damage Detection*

The SSI/Principal Component method implemented in the tool ARTeMIS (SVS, 2006) was used to estimate the modal parameters for all the fourteen DS. As an example of the frequency shifts along the DS, Table 3 presents for the Test Series C (the last series) the frequency results for ambient excitation. The frequency values are presented together with the value $\pm 2\sigma_\omega$ as a 95% confidence interval, and the frequency differences Δ_ω to the respective Reference Scenario (RS).

Table 3 – Frequency results for ambient excitation [Hz]

Mode		RS_C	$DS_{I\text{-}C}$	$DS_{II\text{-}C}$ †	$DS_{III\text{-}C}$	$DS_{IV\text{-}C}$
1st	ω	3.41	3.46	3.54	2.99	2.81
	2σ	0.45	0.07	0.29	0.05	0.09
	$\Delta\omega$	–	0.06	0.13	–0.42	–0.60
2nd	ω	12.49	12.44	11.72	10.82	9.27
	2σ	0.05	0.07	0.15	0.16	0.2
	$\Delta\omega$	–	–0.05	–0.77	–1.67	–3.22
3rd	ω	18.29	18.24	17.56	16.76	16.03
	2σ	0.12	0.07	0.18	0.19	0.3
	$\Delta\omega$	–	–0.05	–0.73	–1.53	–2.26
4th	ω	35.63	35.38	34.41	33.11	32.52
	2σ	1.12	0.26	0.37	0.33	2.78
	$\Delta\omega$	–	–0.25	–1.22	–2.52	–3.11

† - Damage scenario in which the crack c_3 was identified by visual observation

In general, the significant frequency decrease, i.e. higher that $2\sigma_\omega$ (given in a grey box on Table 3), where around the DS where the crack was visually localized, with exception of mode 1 for Series C, as can be seen in Table 3.

To conclude about the global detection results, it seems that the modal properties of the masonry specimen are sensitive to the damage progress.

5.3.2 *Global Damage Location*

The first methods to be applied here were the non-model based methods, namely the COMAC, PM, MSCM, DIM and SCE. In these methods the curvature mode shape values close to zero were neglected in order to avoid noise contamination in the results. The methods were applied only for the case of random impact excitation.

Concerning the performance of the non-model based methods, the PM calculated for modal curvatures, the MSCM, the DIM and the SCE gave similar results, with better agreement for the last three methods. They were able to locate the damage in the vicinity of the experimental crack locations.

The results combination of the selected methods is extensively presented elsewhere (Ramos, 2007). As an example, Figure 11 shows the locations results for the case of the last DS when is compared with the preceding one (relative comparison). The damage location is given by the circles.

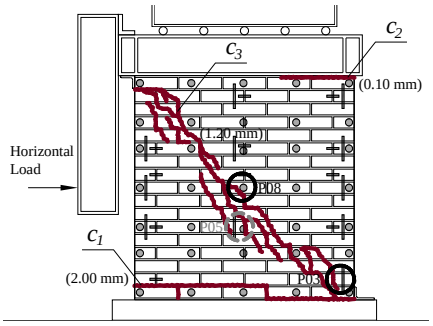

Figure 11 – Combination of non-model based results for the comparison between DS_{III-C} and DS_{IV-C}

The damage localization with FEMU was carried out with an approach similar to the one presented in Section 3.2. For the case of Series C, eight thin bands of elements and one square of elements with different Young's modulus as updating parameter were considered. Figure 12 shows the selected bands together with the final crack pattern.

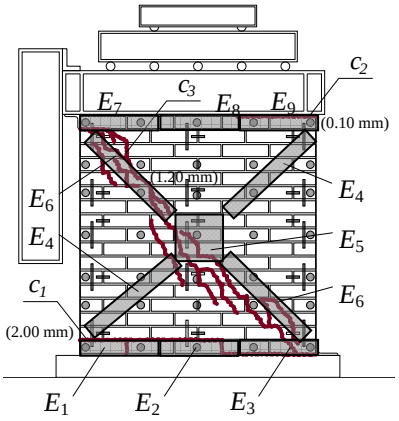

Figure 12 – Updating parameters for the damage analysis

In this series, the damage was expected to be localized at position E_5 and E_6 (crack c_3) and it was also expected to observed the crack growth at positions E_8 and E_9 (crack c_2). Table 4 presents the relative values for the updating parameters, when compared to the values obtained for the same type of analysis but calculated to the RS_C.

Table 4 – Relative values for the updating parameters

Up	DS_{II-C}	DS_{III-C}	DS_{IV-C}
E_1	1.00	0.98	1.00
E_2	1.00	1.00	1.00
E_3	1.00	1.00	1.00
E_4	1.00	0.53	0.01
E_5	0.07	0.05	0.01
E_6	1.00	0.08	0.01
E_7	0.91	0.85	0.51
E_8	0.03	0.09	0.29
E_9	0.69	0.78	0.36

The damage pattern was obtained with the updating analysis DS_{II-C} and DS_{III-C}. In the last updating analysis (DS_{IV-C}) the results were not consistent with the observed cracks, as damage at position E_4 was also pinpointed. This might be related to the large differences between the RS_C and the last DS of test Series C.

6 CONCLUSIONS

In this paper a methodology was proposed based on vibration measurements to identify damage in masonry-like structures. The methodology was then applied to the Clock Tower of Mogadouro, Portugal, and to a laboratory wall specimen.

From the presented analyses, it seems that the proposed methodology is useful and applicable to historical masonry structures. The natural frequency observation seems to be a reliable approach for damage detection, while the mode shape curvatures changes are reliable quantities in the case of damage localization.

7 PREFERENCES

Chang, P.C.; Flatau, A.; and Liu, S.C. 2003. Review Paper: Health Monitoring of Civil Infrastructure, Structural Health Monitoring, Vol. 2 (3), pp. 257-267

Choi, S.; Park, S.; and Stubbs, N. 2005. Non-destructive Damage detection in Structures using Changes in Compliance, International Journal of Soils and Structures, n.42, pp. 4494-4513

DIANA 2006. DIANA-9 Finite Element Analysis, User's Manual - Release 9, TNO, Netherlands

Doebling, S.W.; Farrar C.R.; Prime, M.B.; and Shevitz D. 1996. Damage identification and health monitoring of structural and mechanical systems from changes in their vibration characteristics: a literature review, Los Alamos National Laboratory, NM, 132 p.

Doherty, J.E. 1987. Nondestructive Evaluation, Handbook on Experimental Mechanics, A.S. Kobavashi Edt., Society for Experimental Mechanics

Farrar, C.R. and Doebling, S.W. 1998. Damage Detection and Evaluation II – Field Applications to Large Structures, Modal Analysis and Testing, Júlio Silva and Nuno Maia (Editors), NATO Science Series E, Vol. 363, Kluwer Academic Publishers, London, pp 345-378

Londoño, N.A. 2006. Use of Vibration Data for Structural Health Monitoring of Bridges, PhD Thesis, Carleton University, Ottawa, Canada

MATLAB 2006. MATLAB User Manual, Release 7.2, The MathWorks, USA

Montalvão, D.; Maia, N.M.M.; and Ribeiro, A.M.R. 2006. A Review of Vibration-based Structural Health Monitoring with Special Emphasis on Composite Materials, The Shock and Vibration Digest, Vol. 38, No. 4, pp. 295-324

Peeters, B. 2000. System Identification and Damage Detection in Civil Engineering, PhD Thesis, Catholic University of Leuven, Belgium

Peeters, B.; and De Roeck, G. 1999. Reference-Based Stochastic Subspace Identification for Output-Only Modal Analysis. Mechanical Systems and Signal Processing, 13(6), pp. 855-878

Ramos, L.F. 2007. Damage Identification on Masonry Structures Based on Vibrations Signatures, PhD Thesis, University of Minho, Portugal (www.civil.uminho.pt/masonry)

SVS 2006. ARTeMIS Extractor Pro User Manual, Release 3.5, Structural Vibration Solutions, Aalborg, Denmark